IEEE Access
Multidisciplinary | Rapid Review | Open Access Journal

Received January 20, 2020, accepted February 5, 2020, date of publication February 11, 2020, date of current version February 20, 2020.

*Digital Object Identifier 10.1109/ACCESS.2020.2973273*

# Tone-Mapping Using Perceptual-Quantizer and Image Histogram

**ISHTIAQ RASOOL KHAN, WAJID AZIZ, AND SEONG-O. SHIM**
College of Computer Science and Engineering, University of Jeddah, Jeddah 23218, Saudi Arabia

Corresponding author: Ishtiaq Rasool Khan (irkhan@uj.edu.sa)

This work was supported in part by the Deanship of Scientific Research (DSR), University of Jeddah, under Grant UJ-02-031-DR.

**ABSTRACT** A new tone-mapping algorithm is presented for visualization of high dynamic range (HDR) images on low dynamic range (LDR) displays. In the first step, the real-world pixel intensities of the HDR image are transformed to a perceptual domain using the perceptual-quantizer (PQ). This is followed by construction of the histogram of the luminance channel. Tone-mapping curve is generated from the cumulative histogram. It is known that histogram-based tone-mapping approaches can lead to excessive stretching of contrast in highly populated bins, whereas the pixels in sparse bins can suffer from excessive compression of contrast. We handle these issues by restricting the pixel counts in the histogram to remain below a defined limit, determined by a uniform distribution model. The proposed method is compared with state-of-the-art algorithms, using some well-known metrics that quantify the quality of tone-mapped images, and is found to have the best performance.

**INDEX TERMS** Image enhancement, high dynamic range imaging, tone-mapping, image visualization.

## I. INTRODUCTION

High dynamic range (HDR) images and video have gained much popularity in recent years due to advancements in enabling technologies of capture and display. HDR images not only provide more realistic and engaging visual experience, they also enhance accuracy of scene analysis and recognition tasks. Despite recent popularity of HDR displays, LDR displays still retain a significantly larger share of the consumer market. Moreover, the projectors and printers are still LDR at large, and even the dynamic range of available HDR displays is generally lower than that of the HDR contents. Therefore, compression of the dynamic range of HDR image/video is often required to visualize on screen or paper. This process of matching the dynamic range of contents to the displayable range is called tone-mapping.

A plethora of tone-mapping operators (TMOs) has been developed over the past couple of decades. These algorithms are generally classified into two categories – global and local. Global TMOs use monotonically non-decreasing mapping functions, and their operation is reversible to some extent. On the other hand, local operators do not have this restriction of monotonic operation and allow mapping of the same HDR intensity value to different LDR values depending on the pixel intensity values in the local neighborhood. Local operators allow more flexibility and enhancement of local contrast, but they can produce visual artefacts in the tone-mapped images in some cases. Moreover, the local algorithms are computationally more complex in general, and their operations are irreversible. Global operators are more widely used in the industry, mainly due to their reversibility, and simplicity of implementation especially when real-time operation is required.

Tone-mapping can be imagined as a way of distributing a very large number of intensity levels in the scene to a limited much smaller number of display levels. An intuitive way in such ''allocation of resources'' scenarios is to base the decision on population. Not surprisingly, several tone-mapping methods are based on the histogram of HDR pixel intensities. One of the earliest such works was proposed by Larson *et al.* [1]. The authors however found that histogram-based strategy can overly compress some potentially important but smaller regions, and it can be overly generous to large regions which might not actually need many display levels. For example, a uniform blue sky covering half the image certainly does not require half of the total display levels, which a histogram-based strategy would allocate to it. The authors of [1] proposed a scheme that tries to solve this problem by keeping the pixel counts in histogram bins within defined lower and upper bounds.

The associate editor coordinating the review of this manuscript and approving it for publication was Inês Domingues.

Many variants of histogram-based tone-mapping have been proposed [2]–[7]. Husseis *et al.* [2] proposed a new quantizer for tone-mapping based on histogram-equalization, which performed better than the original histogram-based TMO by Larson *et al.* [1]. Duan *et al.* [3] used histogram adjustment to reproduce global contrast followed by an adaptive adjustment of contrast in the local regions. Boschetti *et al.* [4] used contrast limited adaptive histogram equalization technique to obtain local tone-mapping functions, that enhance the contrast both in dark and bright regions. Recently, Khan *et al.* [5] used the threshold-vs.-intensity (TVI) model of the human visual system (HVS) to build a histogram of non-uniform bin-widths for tone-mapping. In their method, the bin-sizes are determined by the TVI model depending on sensitivity of the HVS in each bin. Moreover, the problem of allocation of excessive display levels to the larger regions is solved by excluding the visually indistinguishable pixels from counting. Nguyen *et al.* [6] formed histograms of HDR and LDR images and used an HVS model to minimize the difference between the two to improve the quality of tone-mapped images. Han *et al.* [7] incorporated the effect of ambient light on the HVS in the method of Khan *et al.* [5], to generate tone-mapped images suitable for different viewing environments.

Construction of histogram can be a slow process when image size is large. Scheuermann and Hensley [8] proposed an efficient implementation of histogram construction on the GPU and effectively applied this for to tone-mapping algorithm of Larson *et al.* [1]. Khan *et al.* [5] also implemented their algorithm on the GPU and reported a real-time performance even for the images of very large dimensions. Ambalathankandy [9] implemented a local histogram equalization algorithm for tone-mapping on FPGA with small memory and minimal data access requirements. These implementations make histogram-based global and local methods attractive for real-time tone-mapping applications.

Several other TMOs have been proposed which do not necessarily use a histogram-based approach for distribution of display levels among the pixel clusters. Most of them use some model of HVS to form the transformation curve for matching the dynamic range of scene to the dynamic range of display. Qiao and Ng [10] used localized gamma correction to adjust the contrast and color saturation in different regions for better visualization of dark and bright pixels. Lee *et al.* [11] used $k$-means to divide the image into number of clusters, and adjusted the display gamma value for each cluster separately. Mantiuk *et al.* [12] proposed a constrained optimization model to determine optimum contrast visibility taking ambient illumination and display characteristics into consideration. Lee *et al.* [13] used an optimization model based on retinal sensitivity of the HVS and histogram of the HDR image, to construct an asymmetric Sigmoid curve for tone-mapping. Wu [14] modeled tone-mapping as a constrained optimization problem and used linear programming to get optimal contrast in output images. Dobashi *et al.* [15] proposed a technique to implement local tone-mapping using fixed-point arithmetic only, while keeping the performance in par with the existing algorithms that use floating-point operations. Liang *et al.* [16] proposed a new decomposition model to get the base and detail layers of the HDR image for tone-mapping, and imposed priors on the layers to minimize the halo artifacts in the results.

Recently Rana *et al.* [17] proposed a deep convolutional neural network for tone-mapping of HDR images. The authors collected a large set of tone-mapped images produced by a number of existing TMOs. For each input HDR image, the outputs of all TMOs were compared using an objective quality index, and the one that got the best score was included in the training set. The deep TMO trained using this set of images would supposedly learn the best characteristics of all TMOs, and hence perform better than the existing TMOs on the test images. The experimental results reported by the authors seem to validate this assumption, as the deep TMO got the best average quality score on the test dataset. There have been several other tone-mapping algorithms proposed in last couple of decades [18]–[26], and the topic remains an active area of research even today. A detailed review of the tone-mapping techniques can be found in [27]–[30].

In this paper, we propose a new histogram-based tone-mapping method for HDR images. The perceptual quantizer (PQ) is an emerging non-linear inverse electro-optical transfer function (EOTF) widely adopted by the industry. Studies have shown that the PQ closely simulates the HVS function. In the proposed algorithm, the HDR contents that contain the real-world luminance values are transformed using the PQ curve. This transformation enhances the dark regions and compresses the bright ones, in line with the working of HVS. However, these PQ-mapped contents are still not suitable for viewing and require enhancement of contrast for display on screen. The proposed algorithm constructs histogram of the luminance of the PQ-transformed data, which is used to design the tone-mapping curve. In addition, a simple and effective method to handle the issues of excessive enhancement and compression of contrast is proposed. We perform detailed experimental evaluations using two well-known metrics that show a convincingly better performance of the proposed algorithm compared to the existing state of the art methods.

Rest of this paper is organized as follows. In section II, we explain the proposed tone-mapping algorithm in detail. Section III provides insight of the design parameters and explains the way of choosing their values to get the output images of high quality. Section IV reports the results of experimental evaluations, comparing the quality of outputs of the proposed and some state-of-the-art algorithms. Finally, some conclusions are drawn from this work in section V.

## II. THE PROPOSED TONE-MAPPING ALGORITHM

A flowchart describing the proposed algorithm is shown in Fig. 1, and the main steps are explained below in this section.

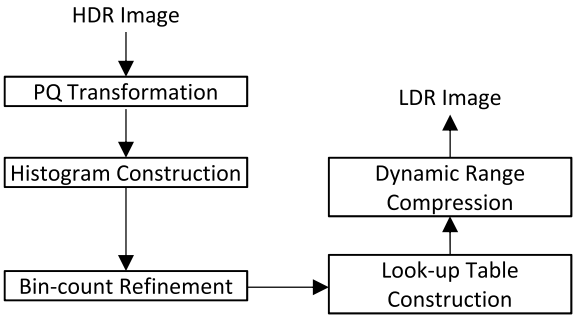


**FIGURE 1.** Flow diagram showing major steps of the proposed tone-mapping algorithm.

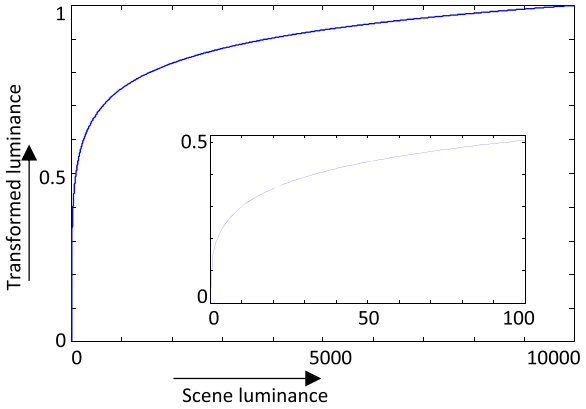


**FIGURE 2.** Perceptual Quantizer (PQ) curve. In the inset, zoomed view of the lower section of the curve is shown.

HDR images capture real-world intensities in units of cd/m$^2$, also called nits. Like LDR images, which are generally transformed with gamma curves for display, HDR images also need transformation. However, due to larger range of intensities that modern displays can reproduce, new EOTF curves are needed for this instead of the traditional gamma curves. The Society of Motion Picture and Television Engineers (SPMTE) published the PQ transfer function in the standard ST.2084, which allows this transformation for the HDR video with maximum luminance level of 10,000 cd/m$^2$. In 2016, the International Telecommunication Union Radiocommunication Sector (ITU-R) released the Recommendation BT.2100[1] which mentions PQ as a transfer function for HDR contents. Unlike gamma curves, which work on relative intensities, PQ maps absolute real-world intensities to the new range. An input luminance value $L_{in}$ in [0, 10000] cd/m$^2$ range is mapped to a new value $L_{out}$ using the following function:

$$L_{out} = \left( \frac{107 + 2413(Lin/10000)^m}{128 + 2392(Lin/10000)^m} \right)^n, \tag{1}$$

where

$$m = \frac{1305}{8192}, \quad n = \frac{2523}{32}.$$

The PQ curve produced by the about equation is plotted in Fig. 2. It can be seen that the transformation enhances the dynamic range of dark regions and compresses that of the brighter regions. In the inset in Fig. 2, zoomed view of the lower section of the PQ curve is shown, which explains that a very small range of input luminance, [0, 100] nits, is expanded to more than 50% of the output luminance range. It has been shown in literature that the HVS works in similar way and the PQ represents it accurately. However, the HDR images transformed with PQ still have very high dynamic range, and therefore do not exhibit good contrast on LDR screens if displayed without further processing. An example is shown in Fig. 3, where an HDR scene "snow" is shown after PQ transformation. For comparison, the final tone-mapped version produced by the algorithm presented later in this paper is also shown. The image processed by the PQ alone appears washed out and has very low contrast comparatively.

In the proposed algorithm, weighted sum of the RGB channels of HDR image is calculated to get the luminance channel as:

$$L = 0.2126R + 0.7152G + 0.0722B. \tag{2}$$

which is transformed using the PQ function given by (1). Histogram of the PQ-transformed luminance channel is formed which groups the pixel intensities in $N$ different clusters. Assuming that $n(m)$ is the number of pixels fallen in bin $m$, where $1 \leq m \leq N$, we form a look up table (LUT) of $N+1$ rows and two columns. The first column comprises the HDR intensity values at the edges of the histogram bins given by:

$$T_i^{(1)} = \min(L) + i \cdot (\max(L) - \min(L))/N, \ 0 \leq i \leq N. \tag{3}$$

The second column of the LUT is calculated as

$$T_i^{(2)} = \begin{cases} 0, & i = 0, \\ T_{i-1}^{(2)} + n(i), & 0 < i \leq N, \end{cases} \tag{4}$$

and then normalized to [0, 255] range as

$$T_i^{(2)} = 255 \cdot T_i^{(2)} \Big/ T_N^{(2)}, 0 \leq i \leq N. \tag{5}$$

Note that the first column of the LUT contains the representative HDR luminance values whereas the second column gives the corresponding LDR values. This LUT can be used to transform all HDR luminance values to LDR using linear interpolation. If a given HDR value $L_{hdr}$ falls into $i^{th}$ interval of the first column of LUT, i.e.,

$$T_i^{(1)} < L_{hdr} \leq T_{i+1}^{(1)},$$

it would map to the following LDR value:

$$L_{ldr} = T_i^{(2)} + \left( T_{i+1}^{(2)} - T_i^{(2)} \right) \cdot \frac{\left( L_{hdr} - T_i^{(1)} \right)}{\left( T_{i+1}^{(1)} - T_i^{(1)} \right)}. \tag{6}$$

[1]Broadcasting service (television) series recommendation BT.2100 by ITU-R specifies various aspects of HDR video.

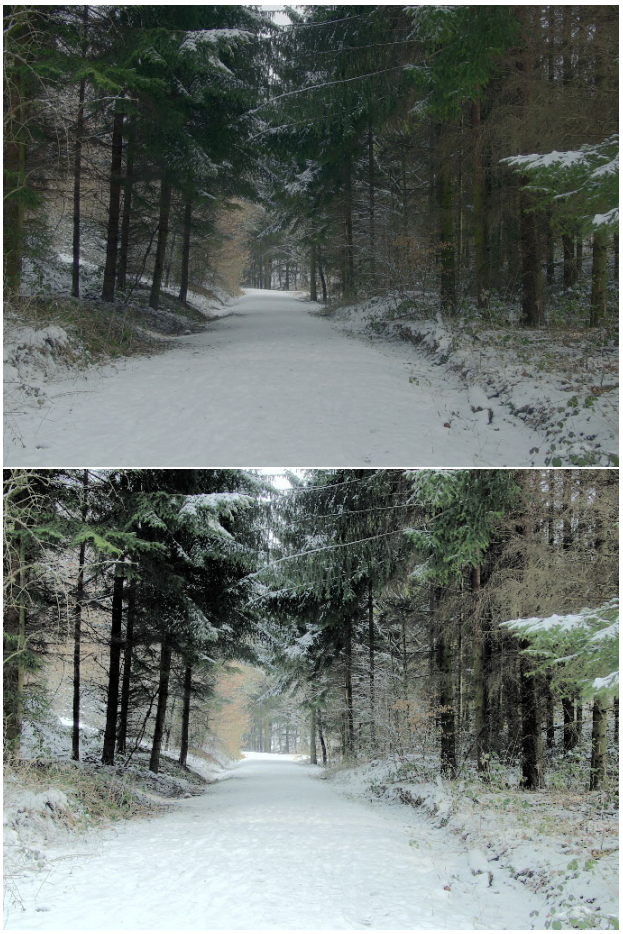

**FIGURE 3.** The HDR image "snow" transformed with PQ (above) and tone-mapped with the proposed algorithm (bottom).

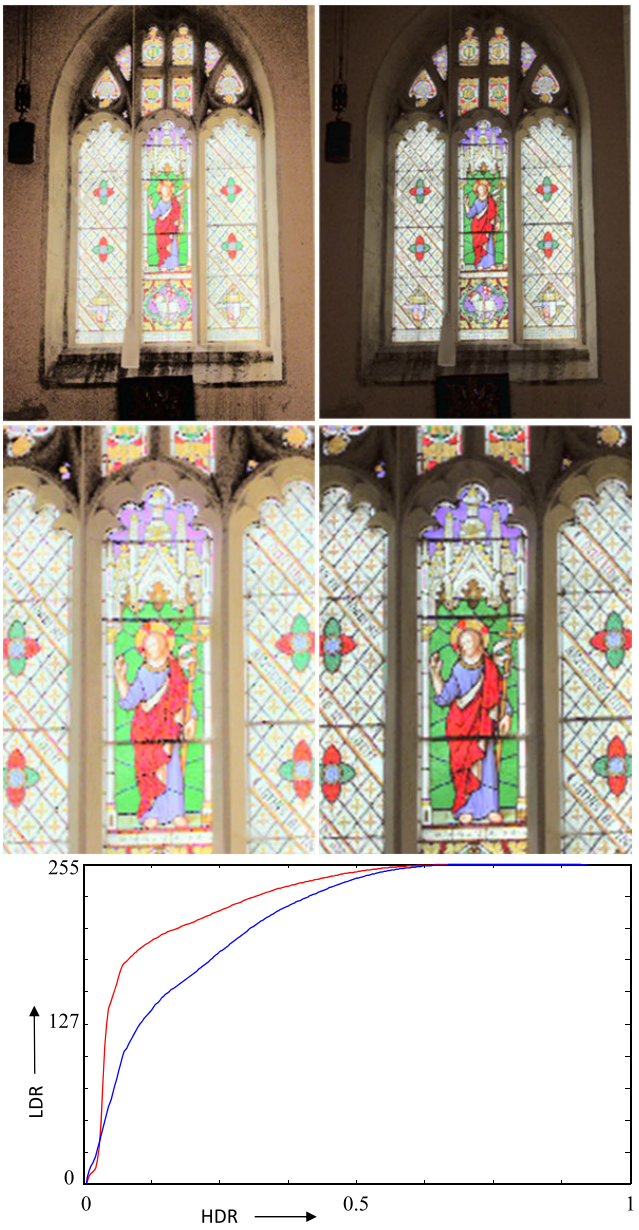


**FIGURE 4.** Effect of histogram count truncation: The red curve is generated without any truncation and produced the image on left. Truncation using $k = 5$ produced the blue curve which generated the image on right. The images in the second row are zoomed views of the middle sections of images.

It was mentioned earlier that histogram-based tone-mapping can lead to over-compression or over-enhancement of some intensity levels, if the pixel counts of the corresponding bins are too small or too large, respectively. To resolve this issue, we impose a limit on the number of maximum pixels in a bin. The idea is similar to the one proposed in [1] in essence, however our technique is different and very simple. If there are $N$ bins, then assuming a uniform distribution of pixel intensities, the number of pixels in each bin would be $1/N$. We set $k/N$ as the value of upper limit on the number of pixels in any bin and truncate larger value of counts to this number. The parameter $k$ has an integer value and will be discussed in detail in the next section. This truncation step significantly improves the quality of the tone-mapped output images. We have shown an example in Fig. 4, where the tone-mapped image produced by our algorithm without truncation of counts is shown on the left. The image on the right is obtained when truncation is done with $k = 5$, which shows better contrast without excessive enhancement or compression in any region. Zoomed views of a small region of both images are shown in the second row of Fig. 4, which demonstrate the effect more clearly. Tone-mapping curves in both cases are also shown in the figure. The red curve that produced the left image is very steep which causes over-stretching of contrast in some regions, whereas the blue curve that generated the right image rises gradually.

Here it should be noted that limiting the number of pixels in a bin means limiting the number of display levels that would be available to that bin. This leaves more display levels for other bins which have smaller pixel counts and would suffer from intensive compression otherwise. Therefore, restricting the maximum number of pixels solves the problems of both over-enhancement and over-compression of contrast.

## III. THE DESIGN PARAMETERS

The design presented above needs selection of two parameters – number of histogram bins $N$, and the truncation factor $k$. Based on our experiments with a large number of HDR images, it was found that quality of the tone-mapped results improves with the number of bins, but the improvement is marginal if the number of bins is already reasonably large. To measure the quality, we used a quantitative metric TMQI, explained later in the next section. Figure 5 plots the average quality index of 42 test images (taken from the accompanying DVD of [27]) tone-mapped with the proposed algorithm, as function of the number of bins. The blue curve represents the case when no truncation of bin counts is done, while the red curve shows the results when counts are truncated using $k = 5$. A comparison of two clearly shows that truncation of counts leads to better quality of the output images. This can also be seen that when the number of bins is large, the raw counts produce nearly the same quality of results as produced with truncated counts. This is because with a large number of bins, the individual bin counts become small and truncation does not change them much. Another important point to note from Fig. 5 is that truncation makes the algorithm less sensitive to the number of bins, and a high quality can be achieved with a much smaller number of bins. A smaller number of bins allows calculation of histogram with improved speed, which can lead to implementations with real-time performance.

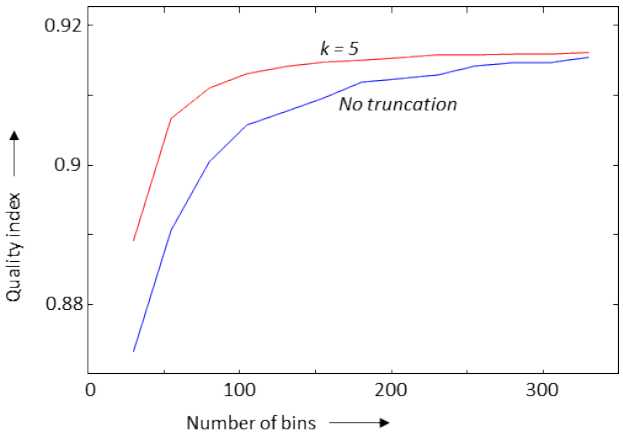


**FIGURE 5.** Mean quality index of 42 tone-mapped images plotted as function of the number of bins.

The second design parameter of the proposed algorithm is the truncation parameter $k$. A larger value of $k$ means a larger threshold values at which the counts will be truncated. To investigate its effect, the average quality scores for the same 42 test images are plotted in Fig. 6. It can be noted that when the number of bins is small, the value of truncation parameter strongly affects the quality. However, when the number of bins is relatively large, the effect of change in this parameter is less profound. A large value of $k$ raises the truncation threshold, making the truncation less likely

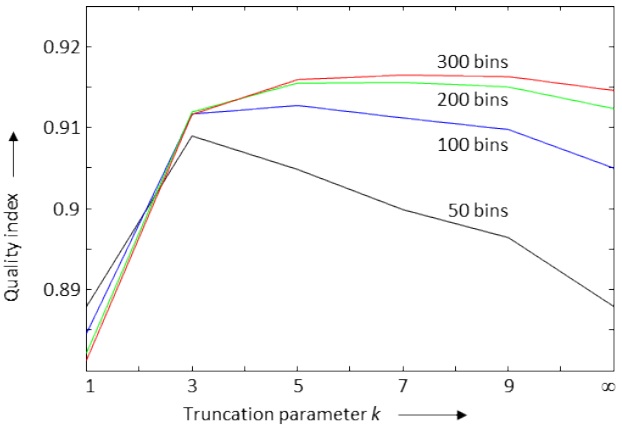


**FIGURE 6.** Mean quality index of 42 tone-mapped images plotted as function of the truncation parameter $k$.

to happen in majority of bins. The value of $k = \infty$ shown in Fig. 6 refers to no truncation. For large number of bins, good quality is achieved even without truncations. Note that the same observation was made above about the curves plotted in Fig. 5.

Here it should be mentioned that the values of parameters $k$ and $N$ that would produce optimal quality outputs can be different for different HDR images. However, performance of the proposed design is not very sensitive to the selected values of these parameters. It can be seen in Figs. 5-6 that for any values of parameters, the quality remains reasonably high. Particularly for $N \geq 100$, any value of $k$ in range of [3], [8] leads to high quality scores. We set the number of bins to 256 and the value of $k$ to 5 as the default parameter values in our implementation. All the results reported in this paper are obtained using these values.

## IV. EXPERIMENTAL EVALUATIONS

We compare our algorithm with three existing state of the art methods – the photographic operator by Reinhard *et al.* [31], the Adaptive TVI-TMO (ATT) by Khan *et al.* [5], and the work of Liang *et al.* [16]. The first algorithm is the most popular TMO due to its simplicity, while the other two are very recent techniques that reportedly produced better results than the previous methods. The first two are global while the third is a local algorithm. The algorithms are implemented using default parameters provided by the authors. For experiments, we use a dataset of 9 EXR images (courtesy Greg Ward) taken from the accompanying DVD of [27]. Tone-mapped versions of these images produced by all four algorithms are shown in Fig. 7. The images produced by the proposed algorithm look quite natural and pleasing across all test images.

For quantitative evaluations, we use a metric called tone-mapping quality index (TMQI) [32], and compare the scores of all four TMOs for the test images. TMQI is a full-reference recently proposed and one of the most popular metrics used to quantify the quality of tone-mapped images. It measures naturalness, structuredness (how good the structure of the

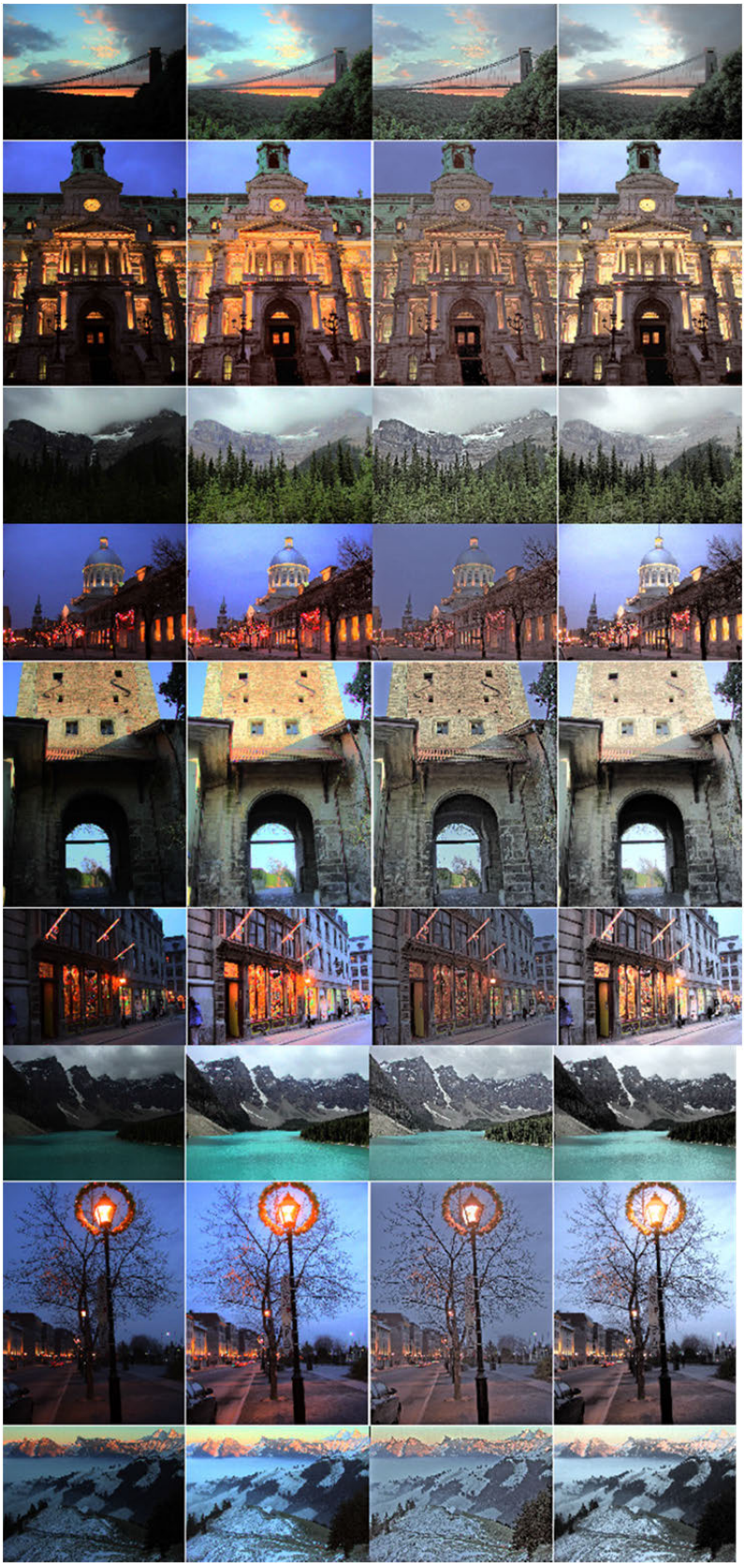

**FIGURE 7.** Outputs of four TMOs on a dataset of 9 HDR scenes (courtesy Greg Ward). Scenes (top to bottom): BristolBridge, ClockBuilding, CrowFootGlacier, DomeBuilding, FribourgGate, MontrealStore, Moraine2, StreetLamp, and Vernicular. Image dimensions: 2048 × 1536 (or 1536 × 2048). TMOs (left to right): Reinhard et al [31], ATT [5], Liang et al [16], and the proposed.

HDR image is preserved after tone-mapping), and overall quality of the results – each scored in [0, 1.0] range, where higher scores indicates better quality. The values of these indexes produced by each algorithm for the test images are given in Table 1, 2 and 3 respectively. Score of the winner in each case is shown in bold, while for the runner-up it is shown in italic. It can be seen that our method stood at the first or the second position for 8 out of 9 times for naturalness, 7 out of 9 times for structuredness, and 8 out of 9 times for quality. On average, it scored highest for all three categories.

**TABLE 1. TMQI scores for naturalness of the tone-mapped images.**

| Image | Reinhard et al. [31] | ATT [5] | Liang et al. [16] | Proposed |
|---|---|---|---|---|
| BristolBridge | 0.0731 | 0.1646 | **0.4546** | *0.2034* |
| ClockBuilding | 0.5689 | *0.8781* | 0.7342 | **0.9424** |
| CrowFootGlacier | 0.1998 | 0.7456 | **0.8954** | *0.8156* |
| DomeBuilding | 0.2405 | **0.5342** | 0.3774 | *0.5306* |
| FribourgGate | 0.5102 | *0.7819* | **0.9571** | 0.7702 |
| MontrealStore | 0.3931 | *0.9372* | 0.3254 | **0.9757** |
| Moraine2 | 0.1382 | 0.3622 | **0.7551** | *0.5256* |
| StreetLamp | 0.4555 | **0.8937** | 0.8262 | *0.8912* |
| Vernicular | 0.4435 | 0.7682 | **0.9277** | *0.8083* |
| AVERAGE | 0.3359 | 0.6739 | *0.6948* | **0.7181** |

**TABLE 2. TMQI scores for structuredness of the tone-mapped images.**

| Image | Reinhard et al. [31] | ATT [5] | Liang et al. [16] | Proposed |
|---|---|---|---|---|
| BristolBridge | 0.8183 | **0.8324** | 0.7997 | *0.8301* |
| ClockBuilding | 0.8509 | *0.8637* | 0.8049 | **0.9025** |
| CrowFootGlacier | 0.8726 | **0.9029** | 0.8846 | *0.8931* |
| DomeBuilding | 0.6878 | **0.8644** | 0.6403 | *0.8576* |
| FribourgGate | *0.9316* | **0.9368** | 0.9251 | 0.9301 |
| MontrealStore | **0.9283** | *0.9204* | 0.9083 | 0.9155 |
| Moraine2 | 0.9114 | 0.9069 | **0.9151** | *0.9146* |
| StreetLamp | 0.8723 | *0.9413* | 0.8612 | **0.9446** |
| Vernicular | 0.9192 | *0.9425* | 0.9058 | **0.9468** |
| AVERAGE | 0.8658 | *0.9012* | 0.8494 | **0.9039** |

**TABLE 3. TMQI scores for quality of the tone-mapped images.**

| Image | Reinhard et al. [31] | ATT [5] | Liang et al. [16] | Proposed |
|---|---|---|---|---|
| BristolBridge | 0.7848 | 0.8129 | **0.8622** | *0.8213* |
| ClockBuilding | 0.8961 | 0.9475 | 0.9096 | **0.9671** |
| CrowFootGlacier | 0.8321 | 0.9381 | **0.9557** | *0.9461* |
| DomeBuilding | 0.7873 | **0.8939** | 0.7991 | *0.8914* |
| FribourgGate | 0.9075 | *0.9524* | **0.9751** | 0.9489 |
| MontrealStore | 0.8858 | *0.9711* | 0.8678 | **0.9753** |
| Moraine2 | 0.8278 | 0.8745 | **0.9428** | *0.9057* |
| StreetLamp | 0.8824 | *0.9701* | 0.9392 | **0.9706** |
| Vernicular | 0.8926 | 0.9518 | **0.9659** | *0.9589* |
| AVERAGE | 0.8552 | *0.9236* | 0.9130 | **0.9317** |

Another well-known objective metric for tone-mapping quality assessment is the "feature similarity index for tone-mapped images" (FSITM) [33]. This metric is based on comparison of the phase-derived feature maps of HDR and LDR images. The authors of [33] suggested to use a combined TMQI-FSITM quality index that achieves better values of Spearman's rank-order correlation coefficient (SRCC) and the Kendall's rank-order correlation coefficient (KRCC) than TMQI and FSITM alone. The TMQI-FSITM scores of the methods being compared here are shown in Table 4 for all the 9 test images. The trend in these results remains the same as for the TMQI based comparisons in Tables 1-3. Our method outperforms others for majority of the scenes. It achieves the best average score, while standing at the first position for five images and second for three.

**TABLE 4. TMQI-FSITM scores of the tone-mapped images.**

| Image | Reinhard et al. [31] | ATT [5] | Liang et al. [16] | Proposed |
|---|---|---|---|---|
| BristolBridge | 0.8141 | 0.8208 | **0.8591** | *0.8501* |
| ClockBuilding | 0.8466 | 0.8767 | 0.8737 | **0.9095** |
| CrowFootGlacier | 0.8578 | 0.9066 | **0.9221** | *0.9131* |
| DomeBuilding | 0.8257 | *0.8668* | 0.8335 | **0.8724** |
| FribourgGate | 0.8610 | 0.9003 | **0.9234** | *0.9082* |
| MontrealStore | 0.8511 | *0.9038* | 0.8642 | **0.9196** |
| Moraine2 | 0.8665 | *0.9061* | **0.9215** | 0.9059 |
| StreetLamp | 0.8620 | *0.9248* | 0.9168 | **0.9371** |
| Vernicular | 0.8672 | 0.9275 | *0.9326* | **0.9366** |
| AVERAGE | 0.8502 | 0.8941 | 0.8926 | **0.9058** |

In a recent trend, deep learning has been used for several image processing applications including tone-mapping [17]. The authors of [17] compared their deep TMO with many existing TMOs using a dataset of 105 HDR scenes available at [34]. They reported that their TMO got the highest average score of TMQI, 0.88. We applied our TMO to the same dataset and got an average score of 0.89, using the default values of design parameters. Other algorithms also got lower average scores than ours as shown in Table 5. This comparison further validates superiority of the proposed TMO over existing state of the art.

**TABLE 5. Average TMQI quality scores of five algorithms for 105 test images taken from [34].**

| Method | TMQI Score (Quality) |
|---|---|
| Reinhard et al. [31] | 0.7542 |
| ATT [5] | *0.8833* |
| Liang et al. [16] | 0.8661 |
| Deep TMO [17] | 0.88 |
| Proposed | **0.8896** |

The proposed algorithm has a simple operation, which can be implemented very efficiently. We compare its computational efficiency with other algorithms in Fig. 8, for the test dataset of 42 images mentioned above. Individual results of some typical images of different sizes are shown in Table 6. Both, the figure and the table show the time taken by each

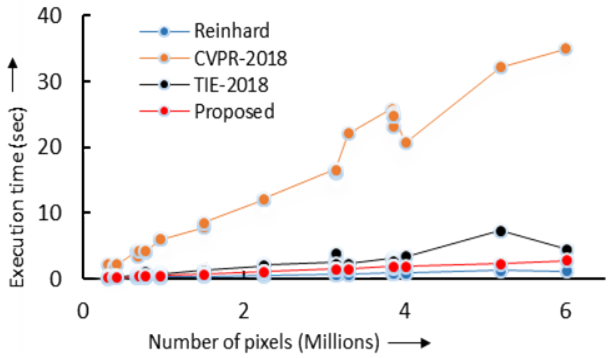


**FIGURE 8.** Time taken for tone-mapping by different algorithms as function of the image size.

**TABLE 6.** Comparison of execusion time of four algorithms.

| Number of Image Pixels (Millions) | Time (seconds) | | | |
|---|---|---|---|---|
| | Reinhard et al. [31] | ATT [5] | Liang et al. [16] | Proposed |
| 0.308771 | **0.1017** | 0.4606 | 2.2755 | *0.1391* |
| 0.667332 | **0.1693** | 0.6054 | 4.1642 | *0.3267* |
| 0.967872 | **0.2306** | 0.7566 | 6.0328 | *0.4480* |
| 1.504000 | **0.3539** | 1.2383 | 7.8027 | *0.7188* |
| 2.252160 | **0.5255** | 2.0280 | 12.0969 | *1.0553* |
| 3.145728 | **0.6922** | 2.2587 | 16.5460 | *1.4745* |
| 4.021248 | **0.8964** | 3.3789 | 20.7374 | *1.8864* |
| 5.193120 | **1.2746** | 7.3100 | 32.1368 | *2.2699* |
| 6.016000 | **1.1929** | 4.5219 | 34.9612 | *2.7305* |
| AVERAGE | **0.6041** | 2.5065 | 15.1948 | *1.2277* |

algorithm for tone-mapping. In the figure, the horizontal axis shows the number of pixels of the input images, and the vertical axis shows the running time. The simulation was carried out on an HP laptop equipped with Intel(R) Core(TM) i7-3740QM 2.7GHz CPU and 8GB RAM, running on 64-bits Windows 7 OS. All algorithms were executed in MATLAB 2013 using the codes of ATT [5] and Liang *et al.* [16] provided by the authors, and the code of Reinhard *et al.* [31] provided in the HDR toolbox by Banterle [35]. It can be seen that the global TMO by Reinhard *et al.* [31], which applies a simple transformation to the image, is the fastest. However, this algorithm is too simple to produce quality results for different types of HDR scenes. In the results shown in Table 1-5, it was at the last position in terms of the quality of results. Especially, for naturalness (Table 1), it scored less than half the score of any other method. Among the rest three, our algorithm has the best speed. It beats ATT [5] by a factor of 2x, and Liang et al. [16] by a factor of 12x approximately. ATT is also based on histogram like our method; however, it uses an iterative method to determine the number of bins, which makes it slow. Moreover, due to this iterative component, its speed is not necessarily a linear function of the size of image. This is the case for Liang *et al.* [16] as well as can be seen in Fig. 8. On the other hand, the proposed method is a single-pass algorithm without any iterations and therefore the time taken to tone-map an image has a linear relation with the size of image

## V. CONCLUSION

A new histogram-based tone-mapping algorithm for HDR images was presented which outperformed some state of the art existing methods in terms of preserving both naturalness and structure. The proposed algorithm has the following major steps: transformation using PQ, histogram construction, histogram refinement, formation of LUT using cumulative histogram, and transformation using linear interpolation. All operations require a single pass without involving any iterative procedures. Therefore, complexity of the algorithm is low and a linear function of the size of image. The steps of the algorithm can be easily implemented on parallel hardware such as the GPU, for real-time operation.

## ACKNOWLEDGMENT

The authors would like to thank Deanship of Scientific Research (DSR), University of Jeddah, for technical and financial support.

## REFERENCES

[1] G. W. Larson, H. Rushmeier, and C. Piatko, "A visibility matching tone reproduction operator for high dynamic range scenes," *IEEE Trans. Vis. Comput. Graph.*, to be published, doi: 10.1109/2945.646233.

[2] A. Husseis, A. Mokraoui, and B. Matei, "Revisited histogram equalization as HDR images tone mapping operators," in *Proc. IEEE Int. Symp. Signal Process. Inf. Technol. (ISSPIT)*, Dec. 2017, pp. 144–149, doi: 10.1109/ISSPIT.2017.8388632.

[3] J. Duan, M. Bressan, C. Dance, and G. Qiu, "Tone-mapping high dynamic range images by novel histogram adjustment," *Pattern Recognit.*, vol. 43, no. 5, pp. 1847–1862, May 2010, doi: 10.1016/j.patcog.2009.12.006.

[4] A. Boschetti, N. Adami, R. Leonardi, and M. Okuda, "High dynamic range image tone mapping based on local histogram equalization," in *Proc. IEEE Int. Conf. Multimedia Expo*, Jul. 2010, pp. 1130–1135, doi: 10.1109/ICME.2010.5583305.

[5] I. R. Khan, S. Rahardja, M. M. Khan, M. M. Movania, and F. Abed, "A tone-mapping technique based on histogram using a sensitivity model of the human visual system," *IEEE Trans. Ind. Electron.*, vol. 65, no. 4, pp. 3469–3479, Apr. 2018, doi: 10.1109/tie.2017.2760247.

[6] N. H. Nguyen, T. Van Vo, Y. Jeong, Y. Moon, and C. Lee, "Optimized tone mapping of HDR images via HVS model-based 2D histogram equalization," in *Proc. Asia–Pacific Signal Inf. Process. Assoc. Annu. Summit Conf. (APSIPA ASC)*, Nov. 2018, pp. 700–704, doi: 10.23919/APSIPA.2018.8659452.

[7] J. Han, I. R. Khan, and S. Rahardja, "Lighting condition adaptive tone mapping method," in *Proc. ACM SIGGRAPH Posters*, 2018, pp. 37:1–37:2, doi: 10.1145/3230744.3230773.

[8] T. Scheuermann and J. Hensley. (2007). *Efficient Histogram Generation Using Scattering on GPUs*. [Online]. Available: https://developer.amd.com

[9] P. Ambalathankandy, "An adaptive global and local tone mapping algorithm implemented on FPGA," *IEEE Trans. Circuits Syst. Video Technol.*, to be published, doi: 10.1109/TCSVT.2019.2931510.

[10] M. Qiao and M. K. Ng, "Tone mapping for high-dynamic-range images using localized gamma correction," *J. Electron. Imag.*, vol. 24, no. 1, Jan. 2015, Art. no. 013010, doi: 10.1117/1.jei.24.1.013010.

[11] J. Lee, R.-H. Park, and S. Chang, "Tone mapping using color correction function and image decomposition in high dynamic range imaging," *IEEE Trans. Consum. Electron.*, vol. 56, no. 4, pp. 2772–2780, Nov. 2010, doi: 10.1109/tce.2010.5681168.

[12] R. Mantiuk, S. Daly, L. Kerofsky, R. Mantiuk, S. Daly, and L. Kerofsky, "Display adaptive tone mapping," in *Proc. ACM (SIGGRAPH)*, 2008, vol. 27, no. 3, p. 1, doi: 10.1145/1399504.1360667.

[13] D.-H. Lee, M. Fan, S.-W. Kim, M.-C. Kang, and S.-J. Ko, "High dynamic range image tone mapping based on asymmetric model of retinal adaptation," *Signal Process., Image Commun.*, vol. 68, pp. 120–128, Oct. 2018, doi: 10.1016/j.image.2018.07.008.

[14] X. Wu, "A linear programming approach for optimal contrast-tone mapping," *IEEE Trans. Image Process.*, vol. 20, no. 5, pp. 1262–1272, May 2011, doi: 10.1109/tip.2010.2092438.

[15] T. Dobashi, M. Iwahashi, and H. Kiya, "A fixed-point local tone mapping operation for HDR images," in *Proc. Eur. Signal Process. Conf.*, Nov. 2016, pp. 933–937, doi: 10.1109/EUSIPCO.2016.7760385.
[16] Z. Liang, J. Xu, D. Zhang, Z. Cao, and L. Zhang, "A hybrid l1-l0 layer decomposition model for tone mapping," in *Proc. IEEE Conf. Comput. Vis. Pattern Recognit. (CVPR)*, Jun. 2018, pp. 4758–4766, doi: 10.1109/CVPR.2018.00500.
[17] A. Rana, P. Singh, G. Valenzise, F. Dufaux, N. Komodakis, and A. Smolic, "Deep tone mapping operator for high dynamic range images," *IEEE Trans. Image Process.*, vol. 29, pp. 1285–1298, 2020, doi: 10.1109/tip.2019.2936649.
[18] T. O. Aydın, R. Mantiuk, and H.-P. Seidel, "Extending quality metrics to full luminance range images," *Proc. SPIE, Hum. Vis. Electron. Imag. XIII*, vol. 6806, Mar. 2008, Art. no. 68060B, doi: 10.1117/12.765095.
[19] F. Durand and J. Dorsey, "Interactive tone mapping," in *Rendering Techniques*. Vienna, Austria: Springer, 2000, pp. 219–230.
[20] F. Hassan and J. E. Carletta, "An FPGA-based architecture for a local tone-mapping operator," *J. Real-Time Image Process.*, vol. 2, no. 4, pp. 293–308, Dec. 2007, doi: 10.1007/s11554-007-0056-7.
[21] A. Benoit, D. Alleysson, J. Herault, and P. Le Callet, "Spatio-temporal tone mapping operator based on a retina model," in *Proc. Int. Workshop Comput. Color Imag.* Berlin, Germany: Springer, Mar. 2009, pp. 12–22.
[22] F. Drago, W. L. Martens, K. Myszkowski, and N. Chiba, "Design of a tone mapping operator for high-dynamic range images based upon psychophysical evaluation and preference mapping," *Proc. SPIE, Hum. Vis. Electron. Imag. VIII*, vol. 5007, pp. 321–331, Jun. 2003, doi: 10.1117/12.473919.
[23] I. R. Khan, "Two layer scheme for encoding of high dynamic range images," in *Proc. IEEE Int. Conf. Acoust., Speech Signal Process. (ICASSP)*, Mar. 2008, pp. 1169–1172, doi: 10.1109/ICASSP.2008.4517823.
[24] K. Kim, J. Bae, and J. Kim, "Natural HDR image tone mapping based on retinex," *IEEE Trans. Consum. Electron.*, vol. 57, no. 4, pp. 1807–1814, Nov. 2011, doi: 10.1109/tce.2011.6131157.
[25] J. Ok and C. Lee, "HDR tone mapping algorithm based on difference compression with adaptive reference values," *J. Vis. Commun. Image Represent.*, vol. 43, pp. 61–76, Feb. 2017, doi: 10.1016/j.jvcir.2016.12.008.
[26] X. Shu and X. Wu, "Locally adaptive rank-constrained optimal tone mapping," *TOGACM Trans. Graph.*, vol. 37, no. 3, pp. 1–10, Jul. 2018, doi: 10.1145/3225219.
[27] E. Reinhard, G. Ward, S. Pattanaik, and P. Debevec, *High Dynamic Range Imaging: Acquisition, Display and Image-Based Lighting*, 2nd ed. San Mateo, CA, USA: Morgan Kaufmann, 2010.
[28] Y. Salih, W. B. Md-Esa, A. S. Malik, and N. Saad, "Tone mapping of HDR images: A review," in *Proc. Int. Conf. Intell. Adv. Syst.*, Jun. 2012, pp. 368–373, doi: 10.1109/ICIAS.2012.6306220.
[29] G. Eilertsen, R. K. Mantiuk, and J. Unger, "A comparative review of tone-mapping algorithms for high dynamic range video," *Comput. Graph. Forum*, vol. 36, no. 2, pp. 565–592, May 2017, doi: 10.1111/cgf.13148.
[30] M. Kumar, B. Chourasia, and Y. Kurmi, "High dynamic range image analysis through various tone mapping techniques," *Int. J. Control Automat.*, vol. 153, no. 11, pp. 14–17, Nov. 2016.
[31] E. Reinhard, M. Stark, P. Shirley, and J. Ferwerda, "Photographic tone reproduction for digital images," *ACM Trans. Graph.*, vol. 21, no. 3, pp. 267–276, 2002, doi: 10.1145/566654.566575.
[32] H. Yeganeh and Z. Wang, "Objective quality assessment of tone-mapped images," *IEEE Trans. Image Process.*, vol. 22, no. 2, pp. 657–667, Feb. 2013, doi: 10.1109/tip.2012.2221725.
[33] H. Z. Nafchi, A. Shahkolaei, R. F. Moghaddam, and M. Cheriet, "FSITM: A feature similarity index for tone-mapped images," *IEEE Signal Process. Lett.*, vol. 22, no. 8, pp. 1026–1029, Aug. 2015, doi: 10.1109/lsp.2014.2381458.
[34] M. D. Fairchild, "The HDR photographic survey," in *Proc. Color Imag. Conf.*, 2007, vol. 2007, no. 1, pp. 233–238.
[35] F. Banterle. *GitHub—Banterle/HDR_Toolbox: HDR Toolbox for Processing High Dynamic Range (HDR) Images Into MATLAB and Octave*. Accessed: Apr. 22, 2019. [Online]. Available: https://github.com/banterle/HDR_Toolbox

**ISHTIAQ RASOOL KHAN** received the B.Sc. degree in electrical engineering from the University of Engineering and Technology, Taxila, Pakistan, in 1992, the M.S. degree in systems engineering from Quaid-i-Azam University, Islamabad, Pakistan, in 1994, and the M.S. degree in information engineering and the Ph.D. degree in digital signal processing from Hokkaido University, Japan, in 1998 and 2000 respectively. He worked at the University of Kitakyushu, Japan, Kyushu Institute of Technology, Japan, Kitakyushu Foundation for the Advancement of Industry, Science and Technology, Japan, Institute for Infocomm Research, A∗STAR, Singapore, and the King Abdulaziz University, Saudi Arabia. He is currently a Professor with the College of Computer Science and Engineering, University of Jeddah. His research interests include high-dynamic range imaging, medical data analytics, and digital signal processing. He was a JSPS Fellow with Hokkaido University, Japan, from 2000 to 2002.

**WAJID AZIZ** received the Ph.D. degree from the Pakistan Institute of Engineering and Applied Sciences (PIEAS), in 2006, and Ph.D. degree from the University of Leicester, U.K., in 2011.

He started his career at the University of Azad Jammu & Kashmir (UAJ&K), in 1998, as a Lecturer. He is currently serving as a Professor with the College of Computer Science and Engineering, University of Jeddah. His core research expertise are in biomedical information systems and his focused areas of research are biomedical signal processing, time series analysis and intelligent data analytics. He has published three books and more than 45 research articles in the reputed national and international journals and conference proceeding. Based on his academic and research contributions, he was a recipient of HEC University Best Teacher Award for the year from 2012 to 2013 by HEC Pakistan, in 2014 and the University Best Teacher Award by the University of AJ&K, in 2013.

**SEONG-O. SHIM** received the B.S. degree in electronics engineering from Ajou University, Suwon, South Korea, in 1999, and the M.S. degree in mechatronics from the Gwangju Institute of Science and Technology, Gwangju, in 2001, and the Ph.D. degree in information and mechatronics from the Gwangju Institute of Science and Technology, Gwangju, in 2011.

He was with LG Electronics DTV Labs, Seoul, Korea, working on research and development of digital TV, from 2003 to 2007. He is currently working as an Associate Professor at the College of Computer Science and Engineering, University of Jeddah, Jeddah, Saudi Arabia. His research interests include computer vision, image processing, 3D shape recovery, and medical imaging.